Original Article

The Therapeutic Role of Stem Cell on Pancreatic Injury Induced by Experimental Hyperthyroidism in Albino Rats (Histological and Immuno histochemical Study)

Karima F. Abdelfadeel, Osama Y. Ibrahim, Mariam A. Abd Elmaksoud and Zeinab M. Alazouny

Department of Medical Histology, Faculty of Medicine, Zagazig University, Egypt

ABSTRACT

Introduction: The adverse effects of hyperthyroidism are related to its duration and the level of thyroid hormone excess. They include cardiac arrhythmias, atrial fibrillation, and even congestive heart failure, renal disorders, and pancreatic injury.

Aim of Work: To assess the harmful effect of hyperthyroidism on the structure of the pancreas of the adult female albino rats and the therapeutic role of human umbilical cord blood mesenchymal stem cells (hUCB-MSCs) as a new strategy in ameliorating pancreatic injury.

Material and Methods: Forty adult virgin female albino rats were assigned to control and treated groups. The treated one was subdivided into hyperthyroid and hyperthyroid + hUCB-MSCs subgroups. Serological analysis was carried out to assess thyroid and pancreatic functions by measuring thyroid-stimulating hormone (TSH), glucose, insulin, amylase levels. Also, anti-oxidant marker as the product of lipid peroxidation malondialdehyde (MDA), and superoxide dismutase (SOD) activity were measured. Pancreatic samples were processed for light microscopic examination. Immunohistochemical examination for insulin protein, caspase-3, PCNA, and CD105 was carried out.

Results: Hyperthyroidism produced biochemical and histopathological alterations in the pancreatic tissue. There was a significant decrease in TSH, serum insulin, serum amylase levels, and SOD enzymes activity but a significant increase in blood glucose and in MDA level in the hyperthyroid group. The acinar cells appeared with vacuolated cytoplasm and dark nuclei. Inflammatory cells, wide septa, and many collagen fibers were noticed. Cytoplasmic immunoreactivity of insulin in beta-cells was reduced; the cytoplasmic reaction of caspase3 was strong in most of the islets and some acini. There were few PCNA positive immunoreactive nuclei in some islet and acinar cells. After hUCB-MSCs injection, the serological and oxidative markers were significantly ameliorated resulting in a nearly normal structure of the pancreas.

Conclusion: Pancreatic tissues were seriously affected by hyperthyroidism with subsequent disturbance in the biochemical markers. Human UCB-MSCs nearly normalized these biochemical and histological changes.

Received: 13 December 2021, **Accepted:** 24 January 2022

Key Words: Hyperthyroidism, pancreas, rats, stem cells.

Corresponding Author: Mariam A. Abd Elmaksoud, MSc, Department of Medical Histology, Faculty of Medicine, Zagazig University, Egypt, **Tel.**: +20 10 6559 6641, **E-mail:** maryam_ahmed17@yahoo.com

ISSN: 1110-0559, Vol. 46, No. 2

INTRODUCTION

Thyroid disorders are one of the most common metabolic disorders which affect women more than men[1]. In hyperthyroidism (HT) or overactive thyroid, the thyroid gland produces high levels of thyroid hormones (THs) [2]. Thyroid hormones have numerous effects on multiple organs of the body. One of these organs is the pancreas that involved in chronic and prevalent diseases, such as diabetes. Furthermore, high levels of THs worsen pancreatic pathology in diabetic patients[3].

The existing relationship between the thyroid gland and the endocrine portion of the pancreas is responsible for the regulation of carbohydrate metabolism. Excess THs stimulate intestinal absorption of glucose and diminish the liver storage capacity of glucose as glycogen. Furthermore, impair pancreatic insulin release, increase peripheral insulin resistance, decrease plasma insulin half-life and increase the catecholamine receptor's expression. Therefore, excess THs produce a diabetogenic effect[4].

Stem cells were used for the treatment of chronic conditions such as diabetes. Stem cells can develop into many other types of cells. They can also renew themselves by division and play an essential role in the regeneration of damaged tissues[5].

Stem cells originated from three sources: embryos, adult body tissues, and birth-related tissues such as placenta, amnion, umbilical cord, and cord blood which are referred to as perinatal stem cells[6]. They have the ability to generate all the cells from the three germ layers. They also have properties of both adult stem cells and embryonic stem cells, with greater pluripotency than adult stem cells, allowing better tissue differentiation capacity as well as multipotent tissue maintenance[7].

 DOI: 10.21608/ejh.2022.111078.1608

Uncontrolled hyperthyroidism adversely affects both patient's quality of life and physical well-being. The ideal treatment for hyperthyroidism is to provide a rapid resolution of symptoms and complications with low complication rates or side effects[8]. So, the aim of this work was designed to assess the harmful effects of hyperthyroidism on the histological and immunohistochemical structure of the pancreas of the adult female albino rats and to evaluate the therapeutic role of hUCB-MSCs as a new strategy in ameliorating pancreatic injury.

MATERIALS AND METHODS

Chemicals

(1) L-Thyroxine (L-T4): One tablet (100µg) was liquified in 1ml distilled water to obtain a solution in which each 1ml contains 100 µg L-thyroxine.

L-thyroxine (100µg) tablets and (5mg) were purchased from GlaxoSmithKline at first section City Centre, Cairo, Egypt.

(2) Labeled Human umbilical cord blood mesenchymal stem cells (hUCB-MSCs): suspended in phosphate buffer solution (PBS) were purchased from the laboratory of Medical Biochemistry and Molecular Biology Department, Faculty of Medicine, zagazig University.

Immunophenotype characterization of hUCB-MSCs

Flow cytometric analysis was done for anti-CD90 (MSC markers) and anti-CD38 (a hematopoietic and endothelial cell marker) to evaluate the immunophenotype of hUCB-MSCs, at the Department of Clinical Pathology, Faculty of Medicine, Zagazig University. In brief, washing the cell suspension with a combination of PBS and 0.1% bovine serum albumin, after trypsinization. A FACScan flow cytometer (Becton Dickinson, Heidelberg, Germany) was used to measure each antibody and culture after incubation for one hour in the dark (Figure A).

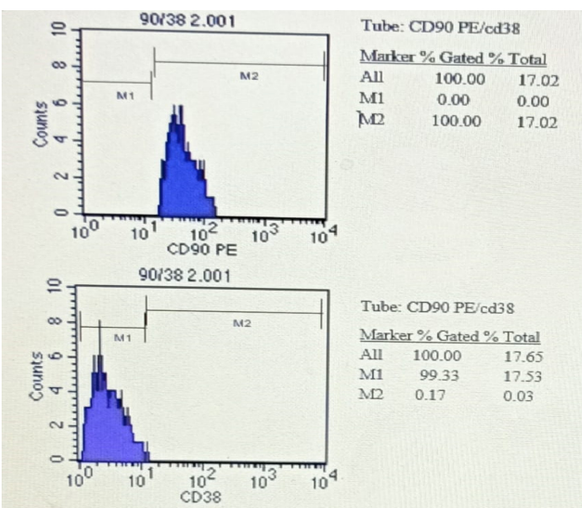

Fig. A: Flow cytometer analysis of hUCB-MSCs showing expression of CD90, but don't express CD38

Detection of homing of stem cells

According to the manufacturer's protocol, hUCB-MSCs were labeled with the red fluorescent dye PKH26 (Sigma Aldrich). In brief, the detached stem cells were washed with PBS and suspended in 1 ml of dilution buffer. The cell suspension was mixed with an equal volume of the labeling solution containing PKH26 and incubated for 5 min at room temperature. Then cells were washed 3 times with the DMEM solution. Fluorescence-labeled hUCB-MSCs were injected intravenously to rats of the hyperthyroid group treated with hUCB-MSCs. Fluorescence microscopic examination (Olympus BX50F4, NO.7M03285, Tokyo, Japan) was done to identify engrafted hUCB-MSCs in pancreatic tissue at the Department of Medical Biochemistry and Molecular Biology, Faculty of Medicine, Zagazig University. The examination revealed the presence of abundant PKH-26 labeled hUCB-MSCs and the positive fluorescent cells appeared scattered and didn't form masses (Figure B).

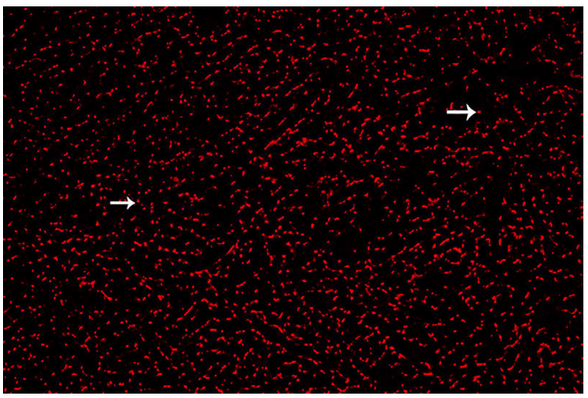

Fig. B: Photomicrographs of fluorescence microscope of rat pancreases after stem cells injection showing abundant hUCB-MSCs labeled with PKH-26 (a red fluorescent dye) appear as sporadic positive fluorescent cells that don't form masses (arrow) (X 200)

Experimental animals

This work was performed on forty adult virgin female albino rats. Their weight was about 180–200gm, aged 10-18 weeks. The animals were obtained from the Breading Animal House, Faculty of Medicine, Zagazig University. They were kept at room temperature with normal light/dark cycles with free access to food and water ad-libitum. They were adapted for two weeks to their environment before starting the experiment. The recommendations of the Institutional Animal Care and Use Committee were fulfilled and accepted by the Faculty of Medicine; Zagazig University.

Experimental design

The rats were divided into two groups:

Group I (control): including 20 rats that were divided into two subgroups, each included 10 rats:

Subgroup Ia (negative control): the rats were left without intervention to measure the basic parameters for four weeks.

Subgroup Ib (vehicle L-T4 and injection): in which 1ml of distilled water was given daily by oral gavage for four weeks and a single intravenous injection of distilled water was given after two weeks from oral gavage of the distilled water[9].

Group II (treated): including 20 rats that were rendered hyperthyroid by daily oral gavage of L-T4 (600 µg/kg/b.wt.) liquified in distilled water for two weeks[10]. Then randomly, the rats were divided into two subgroups, each included 10 rats:

Subgroup IIa (hyperthyroid group): rats were continued on the same dose of L-T4 for another two weeks after induction of hyperthyroidism.

Subgroup IIb (hyperthyroid + hUCB-MSCs)[9]: rats were subjected to administration of 1×106 hUCB-MSCs once intravenously then rats were sacrificed after two weeks.

General observations

Throughout the experiment, the general appearance and daily food consumption of the rats were observed; rats' mortalities and weight were recorded also.

Serological analysis

At the end of the experiment, serological analysis was carried out for each experimental group. Rats fasted overnight with free access to water. From each anesthetized rat blood samples were collected by a capillary glass tube from the retro-orbital plexuses according to the method described by[11], after coagulation of the samples, the serum samples were separated by centrifugation at 3000 r.p.m for ten minutes then they were stored at -20oC for later estimation of:

Thyroid Function Analysis

The serum level of thyroid-stimulating hormone (TSH) was measured on the first day and after two weeks of L-T4 administration by Rat TSH ELISA kit (LS-F5124, LSBio, North America).

Pancreatic Function Analysis

The fasting serum insulin level was measured using Rat Insulin ELISA kit (RAB0904-1KT, Sigma-Aldrich, Steinheim, Germany). The glucose oxidase method was used to measure the fasting plasma glucose level (Bionime GmbH, Switzerland). Serum amylase was measured using a Rat Pancreatic Amylase kit (LS-F19418-1, LSBio, North America).

Oxidative stress and lipid Peroxidation Analysis

Malondialdehyde (MDA) has been identified as the product of lipid peroxidation. MDA was assessed using thiobarbituric acid reactive substances (TBARS) as described by[12].

Assessment of Antioxidant Status

Superoxide dismutase (SOD) activity was assessed colorimetrically at 610 nm as described by[13].

Light microscope examination

After obtaining blood samples, all animals were euthanized by cutting the aorta after cervical dislocation under pentobarbiturate anesthesia (50 mg/kg/rat)[14]. In order to examine the specimens by light microscope, we performed an incision in the middle of the abdomen, and dissection of the pancreas was carried out. Pancreatic samples were fixed in 10% neutral buffered formalin for 48h then processed to get 5 µm-thick paraffin sections[15]. The following stains were used in this study:

Hematoxylin and Eosin stain[15]: as a routine method for studying the general architecture of the pancreas.

Mallory's trichrome counterstained with Hematoxylin stain[15]: For identification of collagen fibers.

Immunohistochemical examination: Immuno-staining was done using the streptavidin biotin-peroxidase technique for recognition of:

a. Insulin protein: using a mouse anti-insulin monoclonal primary antibody of IgG type (clone K36AC10, product No. I 2018) with a minimum working dilution of 1:1000. It was obtained from (Sigma-Aldrich, Steinheim, Germany).

b. Caspase-3 as a marker for apoptosis: using a rabbit anti caspase 3 monoclonal primary antibody of IgG type (clone 3J16, product No. ZRB2121) with a minimum working dilution of 1:100. It was obtained from (Sigma-Aldrich, Steinheim, Germany).

c. PCNA as a marker for cell proliferation: using a mouse anti-PCNA monoclonal primary antibody of IgG type (clone sc-56; product No. AF488) with a minimum working dilution of 1:200 (Santa Cruz Biotechnology, Santa Cruz, CA, USA).

d. CD105 as a marker for human MSCs: using a rat anti CD105 monoclonal primary antibody of IgG type (clone MJ7/18, Product No NM_001146348.1). with a minimum working dilution of 1:200. It was purchased from (Sigma-Aldrich, Steinheim, Germany).

After deparaffinization of the sections (4 µm) in xylene, they were rehydrated in descending-grades of ethanol, and blockage of endogenous peroxidases was done by immersion in 0.3% hydrogen peroxide (H_2O_2) for ten minutes. Antigen retrieval was done for 15 minutes by microwave oven at 100°C in citrate buffer (pH 6.0). Blocking nonspecific binding was done with 3% bovine serum albumin (Dako Ltd, Cambridge shire, UK) for 30 minutes. Two changes of PBS were prepared to rinse the sections in them and then the sections were incubated overnight at 4 °C with the previously mentioned primary antibodies. A biotinylated anti-rabbit antibody was applied after washing in PBS for ten minutes followed by another ten minutes for a peroxidase-marked streptavidin. using 3, 30-diaminobenzidine (DAB, chromogen) the reaction

was visualized. The PBS was used instead of the primary antibody for incubation of negative control sections. Then the counterstain (Mayer's hematoxylin) was added to the sections which were later dehydrated, mounted, and visualized by a light microscope[16]. This technique was performed at the National Institute of cancer, Cairo University.

Examination and photography

Examination and photography of the sections were done at the Department of Medical Histology and Cell Biology, Faculty of Medicine, Zagazig University. The positive results were detected by:

- Anti insulin: brown coloration of the cytoplasmic granules in B cells of the pancreatic islets and the nuclei appeared blue[17].
- Caspase 3: brown coloration of the cytoplasmic granules in pancreatic islets and acini and the nuclei appeared blue[17].
- Anti PCNA: brown coloration of the nucleus and cytoplasm in pancreatic islets and acini[18].
- Anti CD105: brown coloration of the nucleus and the cytoplasm of some cells[19].

Morphometric study

Stained sections with H&E, Mallory's trichrome counterstained with Hematoxylin, and immunohistochemical staining were morphometrically evaluated by Fiji image J (1.51n, NIH, USA) program in the unit of the image analysis at Department of Pathology, Faculty of Dentistry, Cairo University. The image analyzer consisted of a colored video camera, colored monitor, and an IBM hard disc that was linked to the microscope and controlled by Leica Qwin 500 software. Calibration of the image analyzer was done first automatically to obtain the actual micrometer units from the measurement units (pixels) generated by the image analyzer program.

To estimate, the diameter of rounded islets of Langerhans and rounded pancreatic acini using H&E-stained sections and the area % of collagen fibers using Mallory trichrome counterstained with Hematoxylin sections. Also, immunoreaction distribution of anti-insulin, caspase3, and PCNA using immunohistochemically stained sections. A system of computer image analyzer was used. For each parameter 10 non-overlapping histological fields (all fields have the same diameters) were selected from each slide, using an objective lens of magnification x 40. The mean values for each parameter in different groups were determined.

Statistical analysis

The data collected as body weight, food consumption, biochemical and morphometrical analysis were expressed as mean ± SD (standard deviation) and exposed to one-way analysis of variance (ANOVA) for differences between the mean of different groups using Statistical Package for the Social Sciences (SPSS version 20.0) software for analysis. We carried out a further analysis that compare the parameters of the different groups with each other using the post hoc test. The probability of *p-value* less than 0.05 was considered statistically significant & <0.001 for high significant results for two-tailed tests.

RESULTS

General observation

Throughout the experiment, the animals of the hyperthyroid group revealed signs of hyperthyroidism including increased appetite, mild diarrhea, irritability, and increased body temperature. While in hyperthyroid + hUCB-MSCs groups, these signs improved. Also, three rats only died from the hyperthyroid group.

After statistical analysis, the bodyweight of the hyperthyroid group showed a significant decrease as compared to the control groups. While the hyperthyroid + hUCB-MSCs group showed a significant increase as compared to the hyperthyroid group (Table 1). The decrease in body weight was associated with a significant increase in food consumption in the hyperthyroid group in comparison to that of control groups. While the hyperthyroid + hUCB-MSCs group showed a significant decrease as compared to the hyperthyroid group (Table 1).

Biochemical results

After 2 weeks of administration of LT4 (600 µg/kg/day), the mean values of serum TSH level were significantly decreased in the hyperthyroid rats in comparison to that of control groups indicating that the model was successful. (Table 2).

Hyperglycemia and decreased insulin level detected in the hyperthyroid group were significantly improved in the hyperthyroid + hUCB-MSCs group (Table 3).

The hyperthyroid group also showed a significant decrease in the mean values of amylase activity in comparison to the control groups that were significantly ameliorated in the hyperthyroid + hUCB-MSCs group (Table 3).

Furthermore, the hyperthyroid group showed a reduction in mean values of the level of serum SOD in comparison to the control groups. It was significantly ameliorated after the injection of hUCB-MSCs. Also, the increased MDA level detected in the hyperthyroid group was significantly improved after injection of hUCB-MSC (Table 3).

Histopathological results

All control subgroups (a and b) were examined by the light microscopic and revealed closely similar results. Therefore, the histological results of subgroup Ia only are reported.

H&E-stain results

Examination of H&E-stained sections of the control rat's

pancreas revealed a well-organized gland that consisted of two different parts: the endocrine (islets of Langerhans) and exocrine. The lobular arrangement of the exocrine part was well-developed with a marked cellular glandular tissue and a less apparent duct system. The lobules were variable in size and separated by thin septa. Ducts and blood vessels were detected in the connective tissue septa (Figure 1a). The exocrine component was arranged into these lobules and formed of closely packed serous acini. The acini were lined by pyramidal cells with apical acidophilic granular cytoplasm and basal basophilic cytoplasm that contained rounded vesicular nuclei and the lumen was difficult to be observed. The lobules also contained pale areas (islets of Langerhans). The islets of Langerhans were seen interspersed between the acinar cells. They were formed of closely packed irregular cords of cells that had pale rounded nuclei and acidophilic cytoplasm with blood capillaries in between appeared more in the center (Figure 2a).

The pancreas of the hyperthyroid group revealed a loss of its general architecture. The septa were thick. Many blood vessels were congested. The acini were deeply basophilic (Figure 1b). The pancreatic acini were irregularly shaped, and the acinar cells in some lobules were vacuolated and had dark nuclei. Many islets of Langerhans appeared shrunken and lacked the normal smooth demarcation from the acini. They had dark nuclei and vacuolated cytoplasm. (Figure 2b).

After injection of hUCB-MSCs, the pancreas showed apparently normal architecture. The septa were relatively thin and devoid of any infiltrates, congestion in a few blood vessels still present. Ducts detected in the connective tissue septa were relatively normal (Figure 1c). The pancreatic acini and the islet cells appeared normalized. (Figure 2c).

Mallory's trichrome results

Examination of the sections from the control group stained by Mallory's trichrome showed delicate collagen fibers in the thin septa and around the pancreatic acini, the associated blood vessels, and the duct system (Figure 3a). However, the hyperthyroid group showed prominent deposition of collagen fibers especially in the septa, around some pancreatic ducts and blood vessels (Figure 3b). While in the hyperthyroid group treated with hUCB-MSCs little collagen fibers were found in the septa around some pancreatic ducts and blood vessels (Figure 3c).

Immunohistochemical results

Immunohistochemically stained sections for insulin protein revealed strong cytoplasmic immunoreactivity of insulin in beta-cells and negative reaction of the peripheral non-B- cells in the control group (Figure 4a). While the hyperthyroid group showed mild cytoplasmic immunoreactivity of insulin in beta-cells (Figure 4b). Furthermore, the hyperthyroid group treated with hUCB-MSCs showed strong immunoreactivity of insulin in the cytoplasm of beta-cells (Figure 4c).

Immunohistochemically stained sections for caspase 3 in the control group showed mild cytoplasmic immunoreactivity in a few islet cells (Figure 5a). While the hyperthyroid group showed a strong cytoplasmic reaction in most of the islet and some acini (Figure 5b). While the hyperthyroid group treated with hUCB-MSCs showed a mild cytoplasmic reaction in a few islet cells and some acini (Figure 5c).

Immunohistochemically stained sections for PCNA showed positive immunoreactivity in nuclei of a few islet and acinar cells in the control group (Figure 6a). The hyperthyroid group revealed positive immunoreactivity in nuclei of some islet and acinar cells (Figure 6b). While the hyperthyroid group treated with hUCB-MSCs showed nuclear and cytoplasmic immunoreactivity are detected in most islet & acinar cells (Figure 6c).

Immunohistochemically stained sections for CD105 Showed that the control and the hyperthyroid group had negative immunoreactivity in all cells (Figures 7a,b). While the hyperthyroid group treated with hUCB-MSCs showed brown cytoplasmic immunoreactivity in several irregularly shaped cells between and within the acini and the connective tissue septa (Figure 7c).

Morphometric results

Statistical evaluation of the results of H&E-stained sections was done and presented in (Table 4).

Diameter of the islets: When comparing the hyperthyroid group to the control groups, the mean values of the diameter of the islets in random sections indicated a significant decrease in the hyperthyroid group. However, the mean values of the hyperthyroid + hUCB-MSCs group were significantly increased when compared to the hyperthyroid group (Table 4).

Diameter of the acini: When comparing the hyperthyroid group to the control, the mean values of the diameter of the acini in random sections indicated a significant decrease in the hyperthyroid group. However, the mean values of the hyperthyroid + hUCB-MSCs group were highly significantly increased when compared to the hyperthyroid group (Table 4).

The area % of the collagen fibers: When comparing the hyperthyroid group to the control groups, the mean values of the area % of the collagen fibers in random sections indicated a significant increase in the hyperthyroid group. However, the mean values of the hyperthyroid + hUCB-MSCs treated group were significantly decreased in comparison to the hyperthyroid group (Table 5).

The area percent of anti-insulin immuno-reaction: the mean values of the area percent of anti-insulin immuno-reaction in random sections revealed a significant decrease in the hyperthyroid group in comparison to the control groups. However, the mean values of the hyperthyroid + hUCB-MSCs group were significantly increased in comparison to the hyperthyroid group (Table 6).

The area percent of anti-caspase 3 immuno-reaction: the mean values of the area percent of anti-caspase 3 immuno-reaction in random sections when comparing the hyperthyroid group to the control groups revealed a significant increase in the hyperthyroid group. On the other hand, they were significantly decreased in the hyperthyroid + hUCB-MSCs group in comparison to the hyperthyroid group (Table 7).

The area percent of anti-PCNA immuno-reaction: the mean values of the area percent of anti-PCNA immuno-reaction in random sections showed a highly significant increase in the area percent of anti-PCNA immuno-reaction after injection of hUCB-MSCs in comparison to the hyperthyroid group (Table 8).

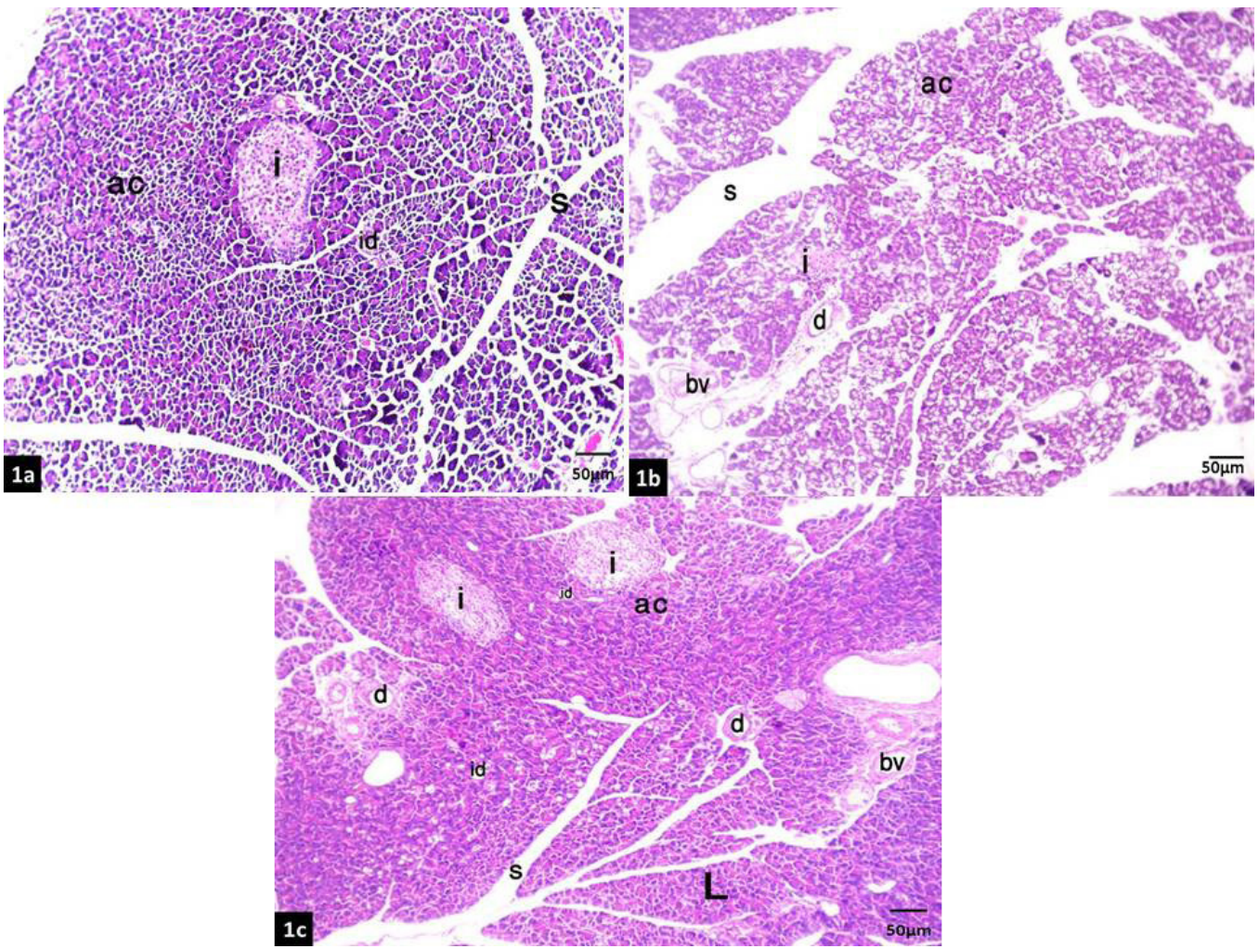

Fig. 1: Photomicrographs of H&E-stained sections of the pancreas of albino rats of the control group (1a): showing its general architecture. It consists of two distinct parts: the exocrine and endocrine (islets of Langerhans). There are multiple thin septa (S) that divide the pancreas into lobules (l). Each lobule is formed of closely packed serous acini (ac). Intra lobular ducts (id) are seen within the lobules. The islets appear lightly stained than the surrounding acinar cells (i). Hyperthyroid group (1b): showing loss of its general architecture. Thick connective tissue septa (s) with congested blood vessels (bv), interlobular ducts (d) are present within it. The pancreatic acini are irregular in shape (ac). Hyperthyroid + hUCB-MSCs group (1c): showing apparently normal architecture with clear separated septa (s) that contain some congested blood vessels (bv). The septa divide it into lobules (l) which contain the islets that appear lightly stained than the surrounding acinar cells (i). (H and E, X100, scale bar 50 um).

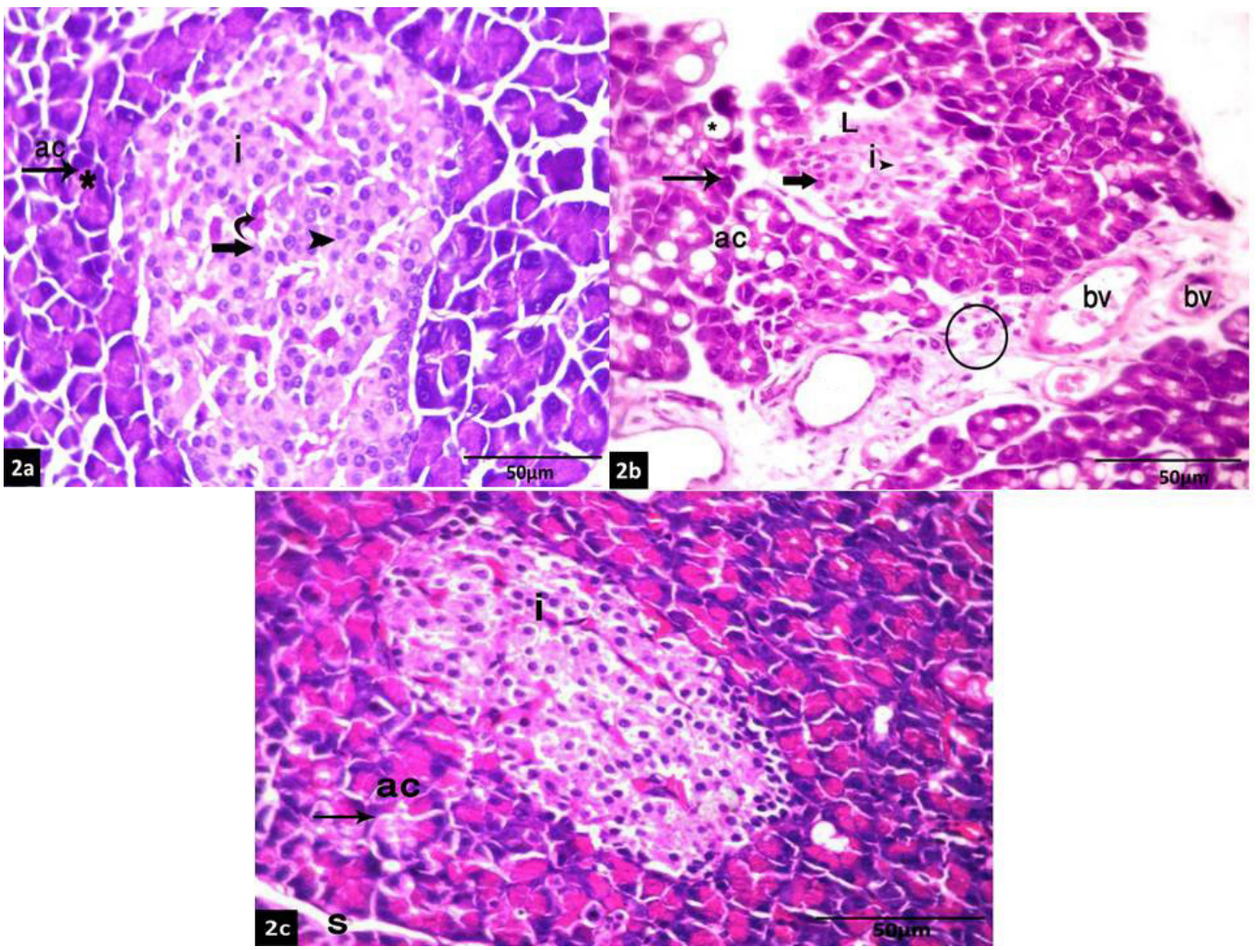

Fig. 2: Photomicrographs of H&E-stained sections of the pancreas of albino rats of the control group (2a): higher magnification showing the serous acini (ac) are lined by pyramidal cells with apical acidophilic granular cytoplasm (*) and basal basophilic cytoplasm (arrow) that contain rounded vesicular nuclei. The cells of the islet (i) appear closely packed irregular cords of cells. They have pale nuclei (thick arrow) and acidophilic cytoplasm (arrowhead) with blood capillaries in between appearing more in the center (curved arrow). Hyperthyroid group (2b): higher magnification of showing inflammatory cells are seen in the thick septum (circle). The blood vessels (bv) are congested. Distorted acini (ac) that are lined by cells with dark nuclei (arrow) and vacuolated cytoplasm (*). The acinar borders are irregular and hardly seen. Shrunken islet (i) is seen. The cells of the islet have irregular outlining (L), dark nuclei (thick arrow), and vacuolated cytoplasm (arrowhead). Hyperthyroid + hUCB-MSCs group (2c): higher magnification showing the pancreatic acini (ac) and the acinar cells with little basal basophilia and oval nuclei (arrow). The islet cells (i) have pale acidophilic cytoplasm and rounded nuclei. (H and E, X400, scale bar 50 um).

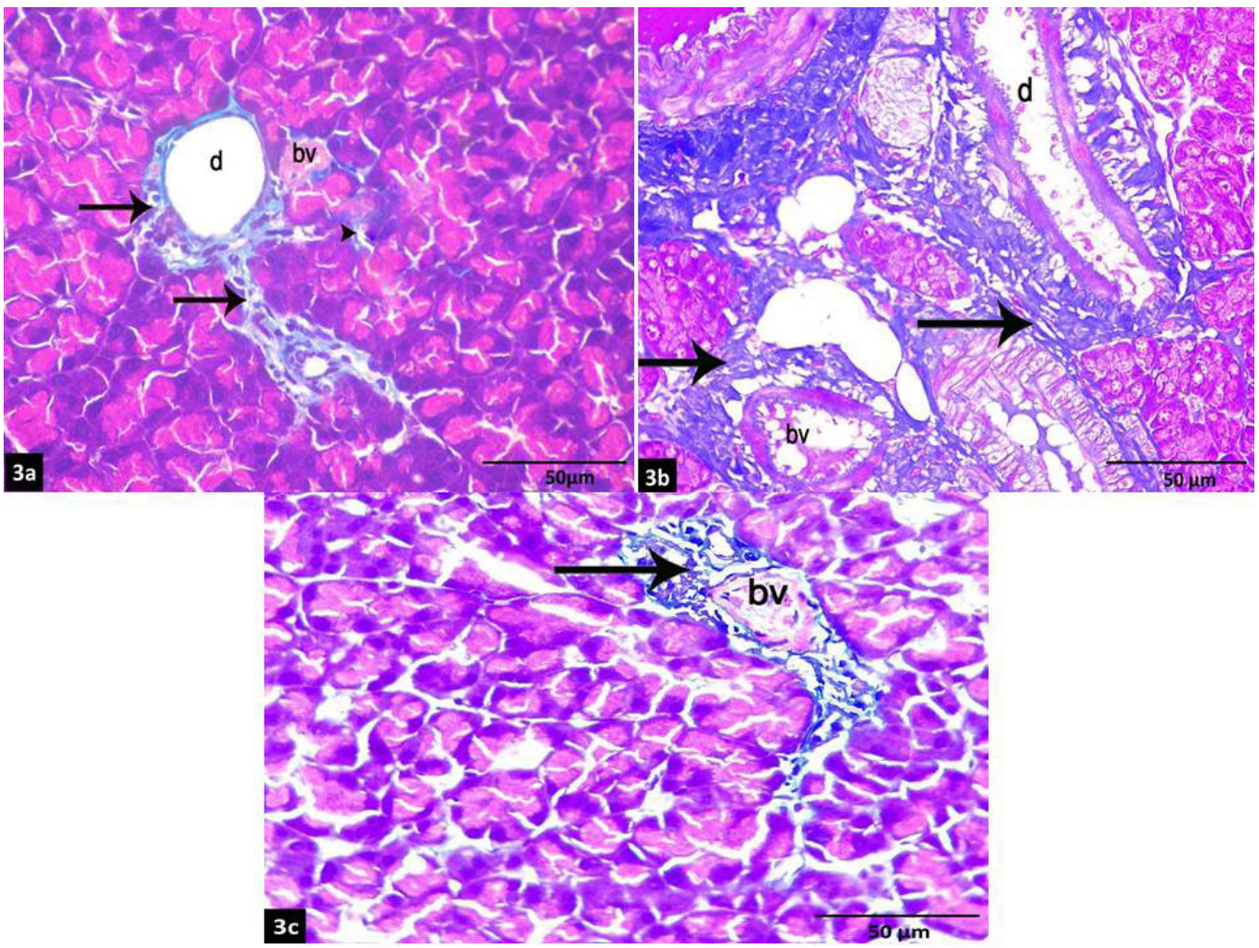

Fig. 3: Photomicrographs of Mallory's trichrome with Hematoxylin counter-stained sections of the pancreas of albino rats of the control group (3a): showing delicate collagen fibers in the thin septa around the pancreatic duct (d), blood vessel (bv) (arrow), and the acini (arrowhead). Hyperthyroid group (3b): showing prominent deposition of collagen fibers (arrow) in the septa, around some pancreatic ducts (d) and blood vessels (bv). [x400]. Hyperthyroid + hUCB-MSCs group (3c): showing little collagen fibers (arrow)in the septa around blood vessels (bv). (Mallory´s trichrome with Hematoxylin counterstain, x400, scale bar 50 um).

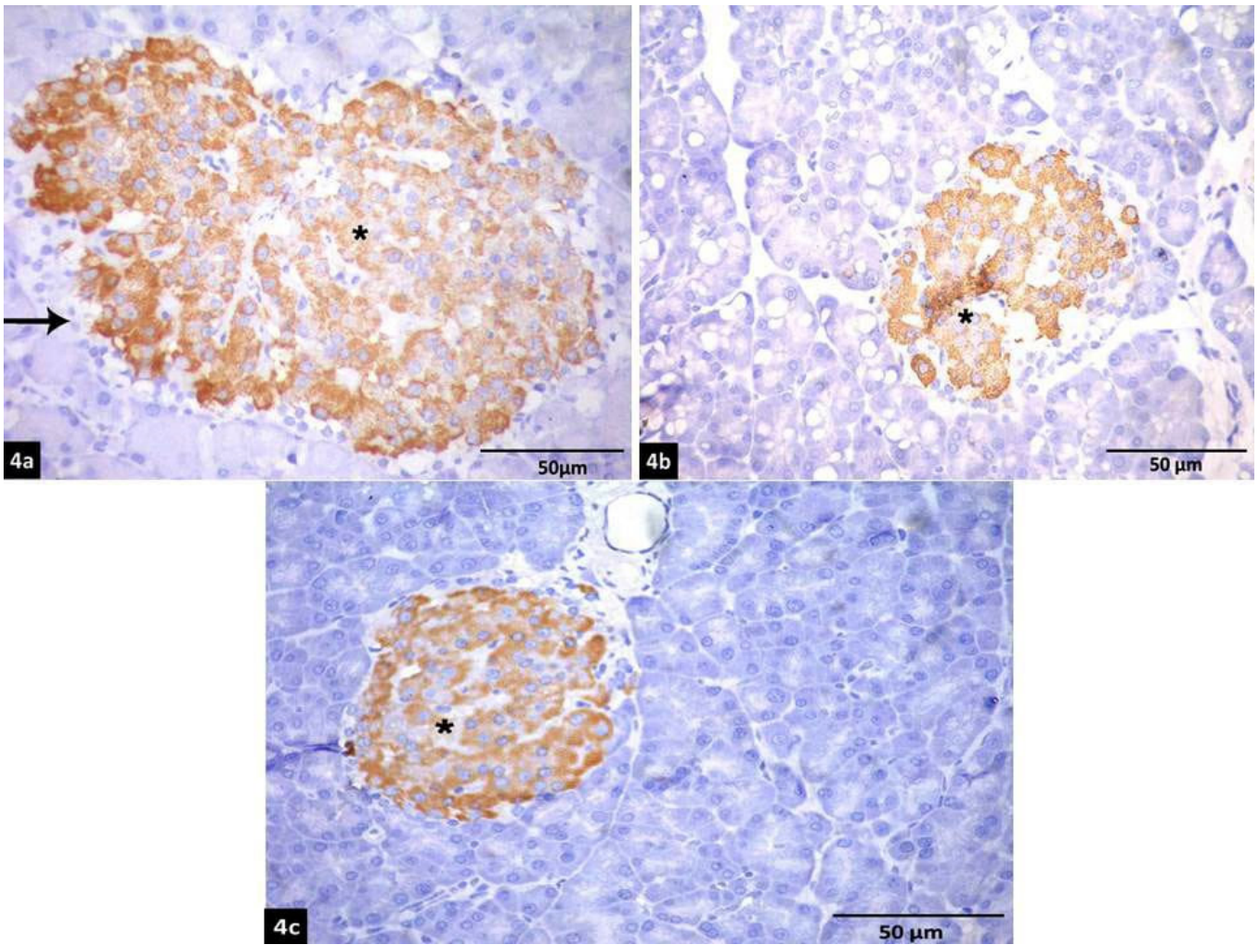

Fig. 4: A photomicrograph of anti-insulin immunohistochemically stained sections in the pancreas of albino rats of the control group (4a): showing strong immunoreactivity of insulin in the cytoplasm of beta-cells (*), which occupy most of the islet. The negative reaction of the peripheral non-B- cells (arrow). Hyperthyroid group (4b): showing mild immunoreactivity of insulin in the cytoplasm of beta-cells (*). Hyperthyroid + hUCB-MSCs group (4c): showing strong immunoreactivity of insulin in the cytoplasm of beta-cells (*). (anti-insulin immunostaining, X400, scale bar 50 um).

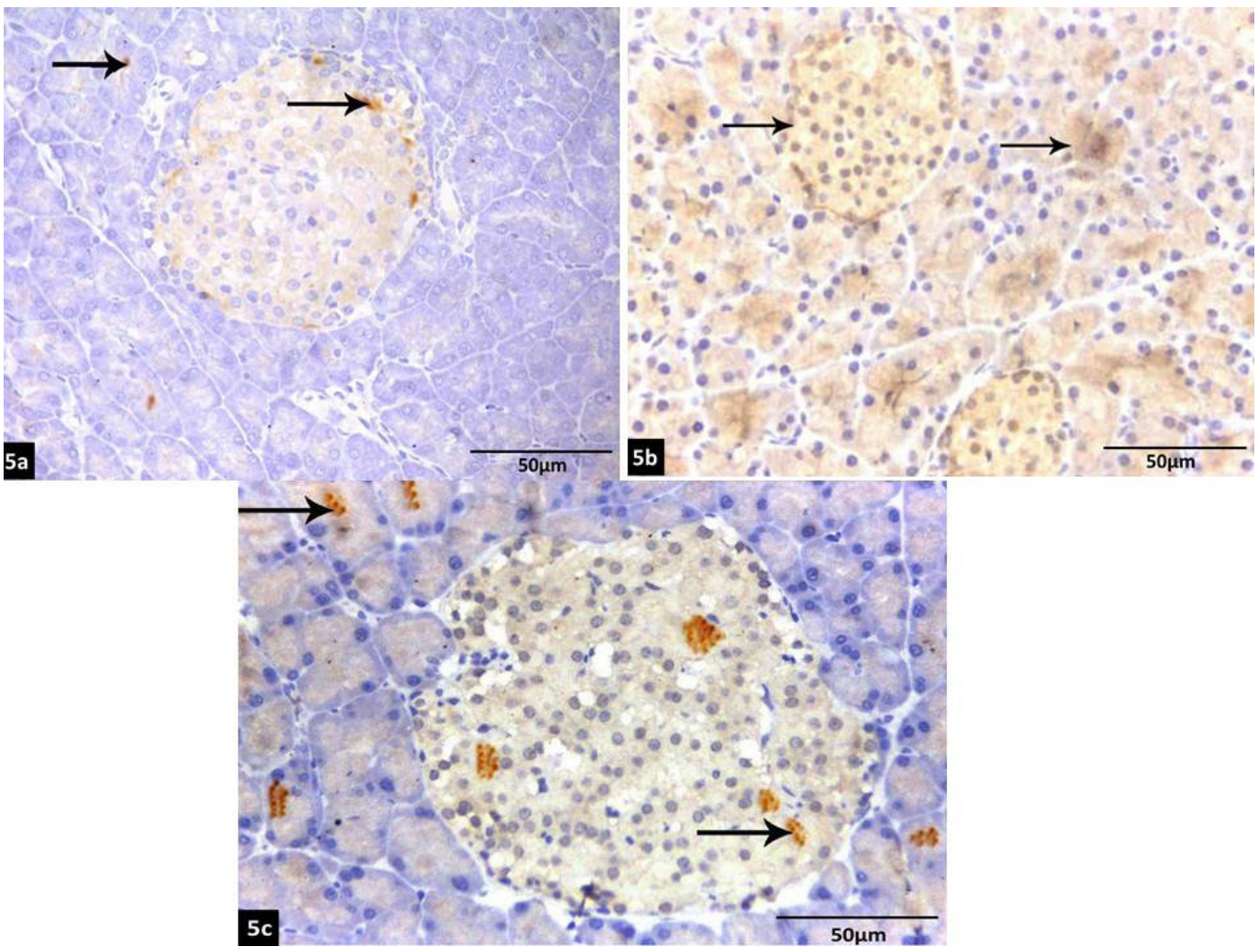

Fig. 5: A photomicrograph of anti caspase3 immunohistochemically stained sections in the pancreas of albino rats of the control group (5a): showing mild cytoplasmic immunoreactivity for caspase 3 in islet and acinar cells. Hyperthyroid group (5b): showing strong cytoplasmic immunoreactivity for caspase 3 in islet and acinar cells. Hyperthyroid + hUCB-MSCs group (5c): showing mild cytoplasmic immunoreactivity for caspase 3 in the islet and acinar cells (arrow). (anti-caspase 3 immunostaining, X400, scale bar 50 um).

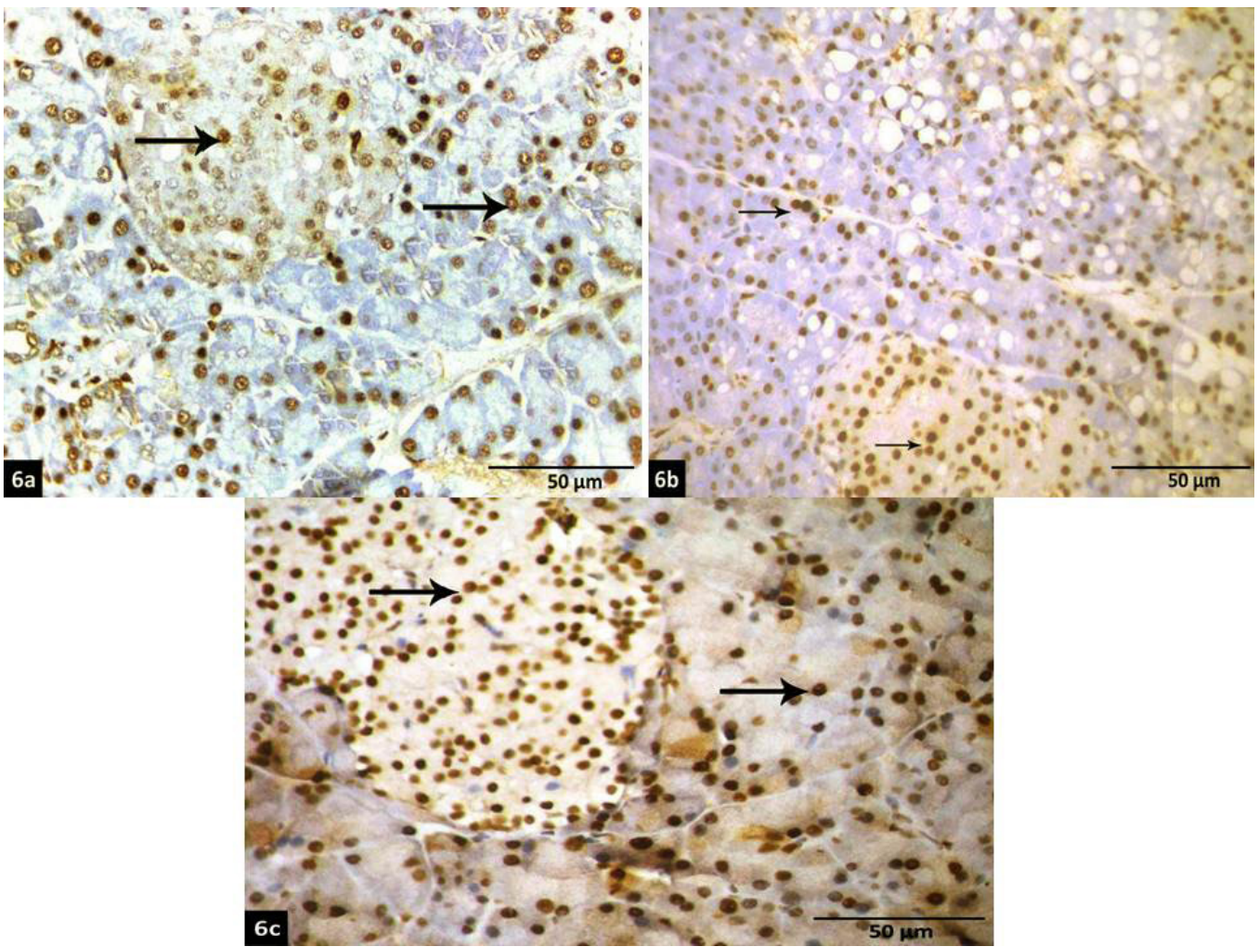

Fig. 6: A photomicrograph of anti PCNA immunohistochemically stained sections in the pancreas of albino rats of the control group (6a): showing positive immunoreactivity for PCNA in the nuclei of a few islet and acinar cells. Hyperthyroid group (6b): showing positive immunoreactivity for PCNA in the nuclei of some islet and acinar cells (arrow). Hyperthyroid + hUCB-MSCs group (6c): showing nuclear and cytoplasmic immunoreactivity for PCN is detected in most islet & acinar cells (arrow). (anti-PCNA immunostaining, X400, scale bar 50 um).

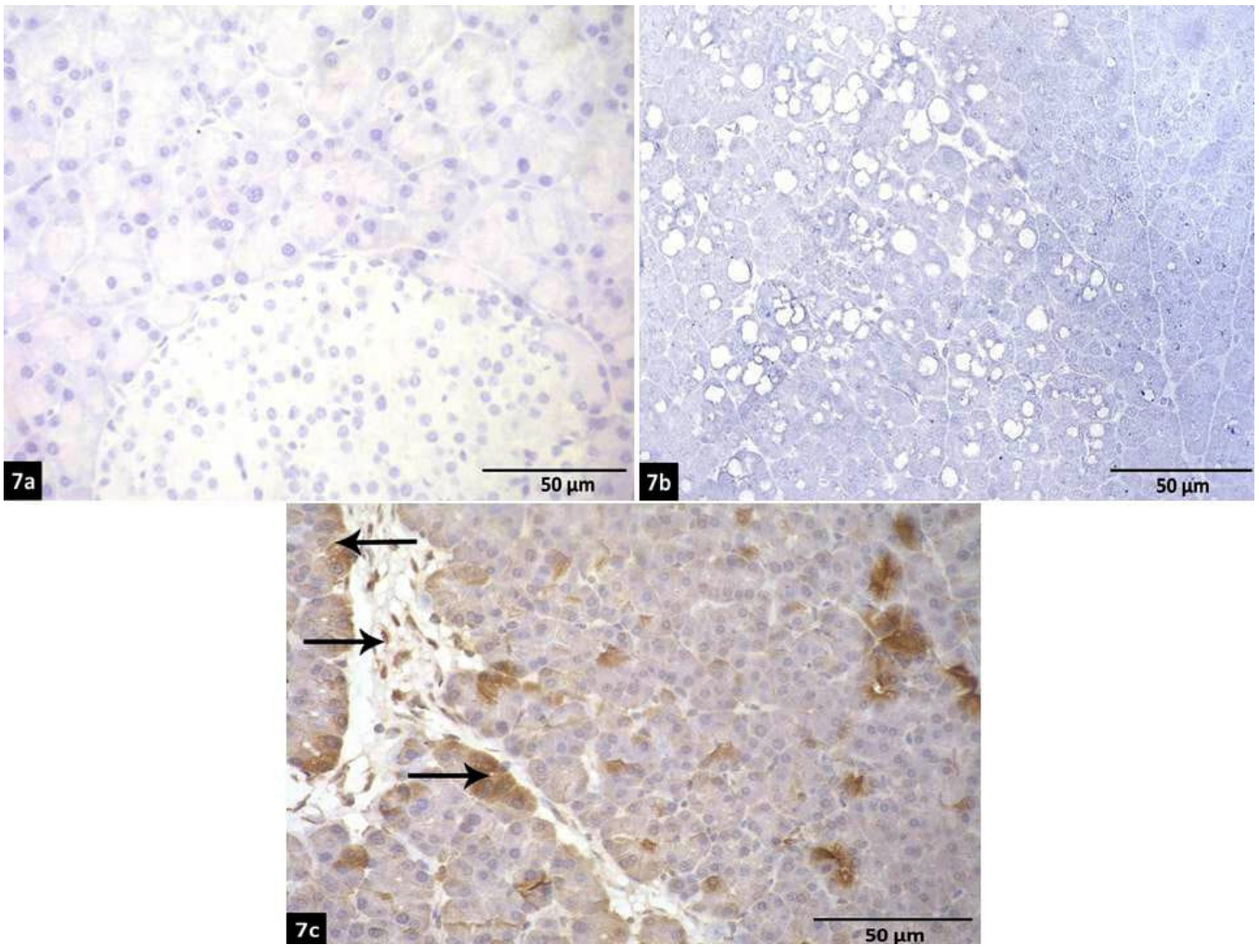

Fig. 7: A photomicrograph of anti-CD 105 immunohistochemically stained sections in the pancreas of albino rats of the control and hyperthyroid groups (7a and b): showing negative immunoreactivity in all cells. Hyperthyroid + hUCB-MSCs group (7c): showing brown cytoplasmic immunoreactivity in several irregularly shaped cells (arrow) within the acini and the connective tissue septum. (Anti-CD105 immunostaining, X400, scale bar 50 um).

Table 1: Body weight & food consumption among the studied groups

Variable	Control groups (N=20)	Hyperthyroid (N=10)	Hyperthyroid + stem cells (N=10)
Body weight (gm): Mean ± SD	225 ± 12.5	160.3 ± 10.8[a*]	225 ± 11.4[b*]
Food consumption (mg/day/rat): Mean ± SD	13.2 ± 0.9	16.7 ± 1.5[a*]	12 ± 1.5[b*]

Data is shown as Mean ± SD.
Significant difference at $p<0.05$.
a : versus control groups.
b : versus the hyperthyroid group.

Table 2: TSH level among the studied groups

TSH(µIU/ml): Mean ± SD	Group I(control) (N=20)	Group II(Treated) (N=20)
In the 1st day	0.08 ± 0.01	0.09 ± 0.02
After 2 weeks	0.08 ± 0.01	0.019 ± 0.002a*

Data is shown as Mean ± SD.
Significant difference at $p<0.05$.
a : versus control groups.

Table 3: Biochemical data among the studied groups

Variable	Control groups (N=20)	Hyperthyroid (N=10)	Hyperthyroid + stem cells (N=10)
Fasting plasma glucose(mg/dl): Mean ± SD	88 ± 2	146.5 ± 8.6^{a*}	91.4 ± 2.3b*
Fasting serum insulin (µIU/ml): Mean ± SD	25 ± 2.3	11 ± 4.3^{a*}	21 ± 2.4^{b*}
Serum amylase (U/l): Mean ± SD	423 ± 3.4	340 ± 9.8^{a*}	410.2 ± 7.2^{b*}
Serum MDA (mmol/l): Mean ± SD	7.9 ± 0.6	15.2 ± 1.6^{a*}	9.2 ± 0.6^{b*}
Serum SOD (U/l): Mean ± SD	8.9 ± 0.8	4.5 ± 0.7^{a*}	8.2 ± 0.3^{b*}

a : versus the control groups.
b : versus the hyperthyroid group.
significant difference (*) (p<0.05).

Table 4: Diameter of islet and diameter of acini data among the studied groups

Variable	Control groups (N=20)	Hyperthyroid (N=10)	Hyperthyroid + stem cells (N=10)
Diameter of islet: Mean ± SD	110.5 ±23.6	28.7 ± 3.5^{a*}	98.2 ± 6.7^{b*}
Diameter of acini: Mean ± SD	44.6 ± 4.7	19 ± 1.4^{a*}	39.3 ± 8.8^{b**}

Data is shown as Mean ± SD.
a : versus the control groups.
b: : versus the hyperthyroid group
significant difference (*) (p<0.05).
highly significant difference (**) (p<0.001).

Table 5: Collagen area percent data among the studied groups

Variable	Control groups (N=20)	Hyperthyroid (N=10)	Hyperthyroid + stem cells (N=10)
Collagen area (%): Mean ± SD	4.8 ±1.2	15.9 ± 2.3^{a*}	6.2 ± 1.5^{b*}

Data is shown as Mean ±SD.
a : versus control groups.
b : versus the hyperthyroid group.
significant difference (*) (p<0.05).

Table 6: Anti-insulin immune reaction data among the studied groups

Variable	Control groups (N=20)	Hyperthyroid (N=10)	Hyperthyroid + stem cells (N=10)
Anti-insulin immune reaction (%): Mean ± SD	16.3 ± 6.5	2.3± 1.4^{a*}	15.4 ± 6.5^{b*}

Table 7: Caspase area data among the studied groups

Variable	Control groups (N=20)	Hyperthyroid (N=10)	Hyperthyroid + stem cells (N=10)
Caspase area (%): Mean ± SD	12.7 ± 1.2	40.5± 8.4a*	14.4 ± 6.2b*

Data is shown as Mean ± SD.
a : versus control group.
b : versus the hyperthyroid group.
significant difference (*) (p<0.05)

Table 8: PCNA area data among the studied groups

Variable	Control groups (N=20)	Hyperthyroid (N=10)	Hyperthyroid + stem cells (N=10)
PCNA (%): Mean ± SD	5.5± 2.2	6.5± 2.8	37.6 ± 3.5^{b**}

Data is shown as Mean ± SD.
a : versus control group.
b : versus the hyperthyroid group.
significant difference (*) (p<0.05)

DISCUSSION

Hyperthyroidism was induced in our experimental model by using L-thyroxine which is a synthetic T4 hormone. Excess administration of L-thyroxine resulted in a suppressed TSH level below the normal and increased the concentration of serum thyroid hormones, indicating induction of a hyperthyroid state. This occurs through hypothalamic-pituitary-thyroid axis activation[20].

We confirmed the development of hyperthyroidism by reduced serum TSH levels in hyperthyroid rats compared to the control rats. American thyroid association and American Association of Clinical Endocrinologists guidelines recommend serum TSH measurement as the single most reliable test to diagnose different forms of thyroid disorders[21].

Adult female albino rats were chosen because the development of hyperthyroidism and its variants is linked to autoimmunity which is more commonly found in females than males. This may be due to genetic, environmental, and lifestyle factors[22].

Throughout the experiment, three rats died in the hyperthyroid group. Mortality from hyperthyroidism is due to cardiovascular and cerebrovascular complications and the risk is highest in people over the age of 75 years[23].

The body weights revealed a significant decrease despite the increase in the food consumption of the hyperthyroid group compared to the control. This observation was in agreement with Messarah *et al*.[24]. Klieverik *et al*.[25] explained the loss of weight by the intensification of

thermogenesis, oxygen consumption, and catabolism which occur in HT.

Levels of blood glucose and serum insulin are generally used as indicators for diabetes and pancreatic functions. In the current work, the fasting blood glucose revealed a significant increase in the hyperthyroid group in comparison to the control groups. This evidenced the occurrence of thyroid diabetes and this observation was in accordance with Pisarev[4] who reported pancreatic lesions after treatment with L-T4 for a prolonged time and irreversible status of diabetes called meta-thyroid diabetes was established.

The Fasting serum insulin level revealed a significant decrease in the hyperthyroid group in comparison to the control group. In hyperthyroidism, impaired insulin secretion was due to a reduction in β-cell mass and abnormality in some parts of the insulin secretory pathway[26].

In the current work, serum amylase activity in the hyperthyroid group revealed a significant decrease when in comparison to the control group. This observation was in accordance with Khodair *et al*.[27] and Barrett *et al*.[28] who correlated this low level of serum amylase with metabolic syndrome and Diabetes mellitus. Also, a low level of serum amylase indicates advanced pancreatic illness-causing wide pancreatic damage.

Oxidative stress is a key process involved in tissue damage. The current work proved that hyperthyroidism induced a significant decrease in the serum level of SOD which is considered the first line of enzymatic antioxidant defense against reactive oxygen species (ROS)[29]. Also, the hyperthyroid group revealed a significant increase in the serum level of MDA which is a lipid peroxidation end product and the main marker for these processes[30]. These results were in accordance with Faried and El-Mehi[17] who linked the hypermetabolic condition in hyperthyroidism with increased free radical formation and lipid peroxidation levels.

In this study, injection of hUCB-MSCs nearly normalized the biochemical changes. This was in accordance with Meng *et al*.[31] who mentioned that acute pancreatitis treated by MSCs showed reduced the levels of serum amylase and MDA and increased the levels of oxidative markers.

Microscope examination of the pancreas of the hyperthyroid group revealed loss of its general architecture. The acinar cells in some lobules were vacuolated and had dark nuclei. This was in agreement with Hassan and Zahran[32] as they found signs of vacuolar degeneration and nuclear changes of the altered spinous cells in tongue mucosa of hyperthyroid rats. Hashem and Saad[33] observed multiple vacuoles in the parotid acini of the hyperthyroid rats and mentioned that lipid peroxidation and oxidative stress that occurred in hyperthyroid led to damage of cell membrane, increase in water content, and hydropic degeneration. Moreover, El Ghamrawy[34] said that many organelles are affected by oxidative stress mainly the mitochondria and endoplasmic reticulum as a result of depriving the cell of energy production and activating the pathway of cell apoptosis.

Previous studies explained the presence of inflammatory cellular infiltrations in connective tissue septa by the movement of fluids and leukocytes from the blood into the extravascular tissue as a reaction of microcirculation in inflammatory conditions as hyperthyroidism which enhances the production of high levels of prostaglandins (PGs) that provoke smooth muscle relaxation followed by sinusoidal dilatation, whereas congestion might be due to loss of fluid from the blood and the vessels became engorged with RBCs[35].

Microscope examination of the pancreas after 2 weeks from hUCB-MSCs injection revealed apparently normal architecture except for a few congested blood vessels. This observation was in agreement with Arafa *et al*.[9].

Jung *et al*.[36] also found that human bone marrow-derived clonal MSCs (hcMSCs) could alleviate the mild and also the severe acute pancreatitis resulting in the recovery of pancreatic function and decrease the expression of inflammatory mediators and cytokines. They detected the hcMSCs in severe acute pancreatitis more than in mild ones. This indicates that the degree of tissue injury may play vital role in the action and migration of hcMSCs to the pancreas.

In the current work, the sections of the pancreas of Mallory's trichrome counterstained with Hematoxylin showed a significant increase in the collagen deposition in the connective tissue septa around the pancreatic acini, ducts, and blood vessels of the hyperthyroid group. While the collagen deposition significantly decreased after 2 weeks from the hUCB-MSCs injection. This was in accordance with Meligy *et al*.[37] who observed a significant increase in the collagen deposition of the hyperthyroid liver. Hegazy *et al*.[38] also found that hyperthyroidism was associated with the deposition of collagen fibers and marked thickness in the capsule of the testes.

Safadi and Friedman[39] mentioned that Fibrosis resulted from activation of stellate cells by ROS and subsequent increase in collagen synthesis and fibrogenesis. The antifibrotic effects of hUCB-MSCs observed in this study were parallel to Lucchesi *et al*.[40] who stated that bone marrow MSCs caused a reduction in cardiac fibrosis by secretion of the antifibrotic hepatocyte growth factor by MSCs.

For immunological identification of B-cells, the insulin hormone is considered an important marker. In our work, the immune-stained sections for insulin of the pancreas of the hyperthyroid group revealed a significant decrease in the immunoreactivity of insulin in the cytoplasm of beta-cells. While, after two weeks from hUCB-MSCs there was a strong immunoreactivity of insulin in the cytoplasm

of beta-cells. This was in accordance with Lucchesi *et al*.[40] who said that increasing glucose levels and free radical generation, as well as loss of antioxidant defenses, resulted in a state of oxidative stress which led to beta cells apoptosis.

In the sequence of programmed cell death or apoptosis, caspase3 is activated initially. Concerning, the hyperthyroid group, the immune stained sections for caspase 3, revealed a strong positive reaction in the cytoplasm of the islet and some acinar cells. While, after 2 weeks from hUCB-MSCs there was a mild reaction in the cytoplasm of islet cells and some acini. This was in accordance with Alnahdi,[41] who found a significant elevation in the activity of the caspase 3, in livers of hyperthyroid rats, and Mousa *et al*.[42] who observed a decrease in the apoptosis and caspase-3 expression in the heart by hUCB-MSCs administration.

Jörns *et al*.[43] clarified that hyperthyroidism led to a high rate of apoptosis in the pancreatic beta cells and the ductal cells which are considered to provide stem cells from which insulin-producing beta cells originate.

In our work, PCNA was used as an indicator of cell proliferation and as a component of the DNA replication and repair mechanism. Concerning the hyperthyroid group, the immune-stained sections of PCNA revealed, few positive immunoreactivities for PCNA in the nuclei of some islet and acinar cells. This was in agreement with Meligy *et al*.[37] who found few PCNA positive cells in livers of hyperthyroid rats.

While 2 weeks after hUCB-MSCs there was strong positive nuclear and cytoplasmic immunoreactivity in most islet and acinar cells. This was in agreement with Tögel *et al*.[44] and Milanesi *et al*.[45] who clarified the increase in cellular proliferation of the pancreatic islets, acini, and blood vessels through a change in the tissue microenvironment which was considered the most important mechanism of action of the mesenchymal stem cells. This change could explain the ability of human MSCs to treat autoimmune diseases.

The MSCs most probably had the ability to stop anti β -cells specific T-cell proliferation in the pancreas. Furthermore, they could protect the newly formed β -cells from destruction by T-cells by immunomodulatory factors release[46]. Bhansali *et al*.[47] added another theory for the pancreatic preservation by the MSCs. It might be via their differentiation into β -cells of islets of Langerhans. This theory was supported by Pagliuca *et al*.[48].

In our work, to assess the migration of injected hUCB-MSCs to pancreatic tissue, we used the fluorescent dye that resulted in presence of sporadic positive fluorescent cells that didn't form masses. This was in accordance with Arafa *et al*.[9] who found similar results. Also, it is important to confirm our findings using specific marker CD105 that was known to be expressed in MSCS according to Zanini *et al*.[49] who found that bone marrow MSCs were positive for some markers such as CD105, CD73, CD90, and CD29. We found that the immunostained sections for CD105 revealed negative reaction in all groups except after 2 weeks from the hUCB-MSCs injection. This group showed brown cytoplasmic immunoreactivity in several irregularly shaped cells between and within the acini and the connective tissue septa. This was in agreement of[19].

CONCLUSIONS AND RECOMMENDATIONS

In conclusion, from this study, it was demonstrated that hyperthyroidism could seriously affect the histological structure of the pancreas with subsequent disturbance in the biochemical markers. Human UCB-MSCs nearly normalized these biochemical and histological changes.

So, we recommended hUCB-MSCs as a new strategy to treat pancreatic injury induced by hyperthyroidism. However, before this line of therapy can be used on humans, large-scale regulated and double-blinded clinical trials with various sizes, dosages, and periods are required. These can guarantee the balance between the therapeutic benefits and any hazardous risks.

ETHICAL APPROVAL

All rats received care according to the standards of the National Guide for Care and Use of Laboratory Animals (NIH Publications No. 8023, revised 1978). The Institutional Animal Care and Use Committee (IACUC), Zagazig University, Egypt approved the design of the experiment.

CONFLICT OF INTERESTS

There areno conflicts of interest.

REFERENCES

1. Al-Tonsi, A. A., Abdel-Gayoum, A. A. and Saad, M. (2004): The secondary dyslipidemia and deranged serum phosphate concentration in thyroid disorders. Experimental and molecular pathology, 76(2), 182-187.
2. Kawthalkar, SH. M. (2018): Essentials of clinical pathology 2nd ed., London, Panama, p p: 151.
3. Chen, C., Xie, Z., Shen, Y. and Xia, S. F. (2018): The roles of thyroid and thyroid hormone in pancreas: physiology and pathology. International journal of endocrinology, 201(8), 1- 14.
4. Pisarev, M. A. (2010): Interrelationships between the pancreas and the thyroid. Current Opinion in Endocrinology, Diabetes & Obesity, 17:437–439.
5. Kern, S., Eichler, H., Stoeve, J., Klüter, H.and Bieback, K. (2006): Comparative analysis of mesenchymal stem cells from bone marrow, umbilical cord blood, or adipose tissue. Stem cells, 24(5), 1294-1301.
6. Hass, R., Kasper, C., Böhm, S. and Jacobs, R. (2011): Different populations and sources of human mesenchymal stem cells (MSC): a comparison of adult and neonatal tissue-derived MSC. Cell Communication and Signaling, 9(1), 12.

7. Carlin, R., Davis, D., Weiss, M., Schultz, B. and Troyer, D. (2006): Expression of early transcription factors Oct-4, Sox-2 and Nanog by porcine umbilical cord (PUC) matrix cells. Reproductive Biology and Endocrinology, 4(1):8.
8. Davis, J. R., *et al*. (2019): Rapid relief: Thyroidectomy is a quicker cure than radioactive iodine ablation (RAI) in patients with hyperthyroidism. World journal of surgery 43(3): 812-817.
9. Arafa, M. A., Gouda, Z. A., El-naseery, N. I., Abdel-Nour, H. M., Hanafy, S. M., Mohamed, A. F., and Abo-Ouf, A. M. (2018): Bone Marrow-Derived Mesenchymal Stem Cells Ameliorate the Pancreatic Changes of Chemically Induced Hypothyroidism by Carbimazole in Male Rats. Cells Tissues Organs, 206(3), 144-156.
10. Ejere, V., Iyikite, C., and Nnamonu, E. I. (2019): Evaluation of Dennettia tripetala Baker F. Leaf Aqueous Extract Effect on Hyperthyroidism in Albino Rats. Journal of Natural Sciences Research, 9(8): 2224-3186.
11. Van Herck, H., Baumans, V., Brandt, C. J. W. M., Hesp, A. P. M., Sturkenboom, J. H., Van Lith, H. A., ... and Beynen, A. C. (1998): Orbital sinus blood sampling in rats as performed by different animal technicians: the influence of technique and expertise. Laboratory Animals, 32(4), 377-386.
12. Yagi, K. (1987): Lipid peroxides and human diseases. Chemistry and physics of lipids, 45(2-4), 337-351.
13. Sinha, A. K. (1972): Colorimetric assay of catalase. Analytical Biochemistry, 47(2), 389-394.
14. Prakoso Y. and Kurniasih K. (2017): Effects of aloe vera cream on skin wound healing in sprague dawley rats: the role of CD4+ and CD8+ lymphocytes. Advances in Health Sciences Research (AHSR), 5:58-63.
15. Suvarna, K. S., Layton, C. and Bancroft, J. D. (2018): Bancroft's Theory and Practice of Histological Techniques E-Book. 8th ed., Elsevier Health Sciences, China. Pp:126-139 and 434-475.
16. Dabbs, D.J. (2019): Diagnostic immunohistochemistry E-Book: Theranostic and Genomic Applications. 5th ed., Elsevier, China. p p 542-580.
17. Faried, M. A. and El-Mehi, A. E. S. (2020): Aqueous anise extract alleviated the pancreatic changes in streptozotocin-induced diabetic rat model via modulation of hyperglycemia, oxidative stress, apoptosis, and autophagy: a biochemical, histological and immunohistochemical study. Folia morphologica, 79(3), 489-502.
18. Stančić, A., Korać, A., Otašević, V., Janković, A. and Korać, B. (2018): The effect of simvastatin in pancreas of diabetic rats. Hrana i ishrana, 59(1), 19-25.
19. Sayed, S. S. and Abd El Aziz, D. H. (2013): The effect of mesenchymal stem cell therapy on ischemia–reperfusion-induced injury of the rat pancreas: a histological and immunohistochemical study. Egyptian Journal of Histology, 36(1), 253-264.
20. Hammad, A. Y., Adam, S. I. and Abdelgadir, W. S. (2021): Comparative Effects of Bisphenol A, Carbimazole and Thyroxine Administration on the Thyroid Gland, Serum Selenium and Iodine Concentration of Wistar Rats. Asian Journal of Research and Reports in Endocrinology, 8-18.
21. Gupta, S., M., Verma, A.K., Gupta, A., Kaur, K. and Singh, (2011): Are we using thyroid function tests appropriately? Indian J. Clin. Biochem., 26: 178-181
22. Li, H. and Li, J. (2015): Thyroid disorders in women. Minerva Med.,106(2):109-14.
23. Osman, F., Gammage, M. D. and Franklyn, J. A. (2002): Hyperthyroidism and Cardiovascular Morbidity and Mortality. Thyroid, 12(6), 483–487.
24. Messarah, M., Saoudi, M., Boumendjel, A., Boulakoud, M. S., and El Feki, A. (2011): Oxidative stress induced by thyroid dysfunction in rat erythrocytes and heart. Environmental toxicology and pharmacology, 31(1), 33-41.
25. Klieverik, L. P., Kalsbeek, A., Ackermans, M.T., Sauerwein, H.P., Wiersinga, W.M. and Fliers, E. (2011): Energy homeostasis and body weight before and after cessation of block and replacement therapy in euthyroid patients with Graves' disease. Int J Endocrinol, 2011:1-7.
26. Karbalaei, N., Noorafshan, A. and Hoshmandi, E. (2016): Impaired glucose-stimulated insulin secretion and reduced β-cell mass in pancreatic islets of hyperthyroid rats. Experimental Physiology, 101(8), 1114-1127.
27. Khodair, A. B. and Al-Sharafi, N. M. N. (2020): Activity of Exocrine Pancreatic Enzymes in Diabetic Female Rats. Prensa Med Argent, 106, 3.
28. Barrett, KE., Barman, SM., Boitano, S. and Brooks, HL. (2012): Gannon's review of medical physiology. (24th edtn), McGraw Hill Professional, United States.
29. Babu, K., Jayaraaj, IA. and Prabhakar, J. (2011): Effect of Abnormal thyroid hormone changes in lipid peroxidation and antioxidant imbalance in hypothyroid and hyperthyroid patients. Int J Biol Med Res 2: 11.
30. Joshi, B., Singh, S., Saini, A., Gupta, S. and Vanishree, B. J. (2018): A study of lipid peroxidation and total antioxidant capacity in hyperthyroid & hypothyroid female subjects. Galore Int J Health Sci Res 3:1–8.
31. Meng, H. B., Gong, J., Zhou, B., Hua, J., Yao, L. and Song, Z. S. (2013): Therapeutic effect of human umbilical cord-derived mesenchymal stem cells in rat severe acute pancreatitis. International journal of clinical and experimental pathology, 6(12), 2703.

32. Hassan, G. S. and Zahran, D. H. (2019): Effects of Experimentally Induced Hyperthyroidism on Rat Tongue Mucosa: Histological and Ultrastructural Study. Life Science Journal, 16(1).

33. Hashem, H. and Saad, S. (2020): Comparative Study of the Effect of Experimentally Induced Hyperthyroidism and on the Parotid Gland in Adult Male Albino Rats. Egyptian Journal of Histology, 43(3), 791-807.

34. El Ghamrawy, T.A. (2015): The effect of liquid diet on the parotid gland and the protective role of L carnitine: immunohistochemical and ultrastructural study. Folia Morphol. 74 (1): 42–49.

35. Rubin, E. (2002): Essential pathology. 3rd ed. Philadelphia: Lippincott William & Wilkins. P.85-88.

36. Jung, K. H., Song, S. U., Yi, T., Jeon, M. S., Hong, S. W., Zheng, H. M., ... and Hong, S. S. (2011): Human bone marrow–derived clonal mesenchymal stem cells inhibit inflammation and reduce acute pancreatitis in rats. Gastroenterology, 140(3), 998-1008.

37. Meligy, F., Hussein, O., Mubarak, H. and Abdel–daim, M. (2018): The possible protective role of omega 3 on liver of L thyroxine treated male albino rats. Histological and immunhistochemical study. Journal of Medical Histology, 2(2), 131-145.

38. Hegazy, A. A., Morsy, M. M., Moawad, R. S. and Elsayed, G. M. (2020): Histological Study on the Effect of Experimentally Induced Hyperthyroidism on Testes of Adult Albino Rats and Possible Ameliorating Role of L-carnitine. Egyptian Journal of Histology, 43(1), 63-74.

39. Safadi, R. and Friedman, S. (2002): Hepatic fibrosis—role of hepatic stellate cell activation. Medscape general medicine, 4(3): p. 27-37.

40. Lucchesi, A. N., Freitas, N. T., Cassettari, L. L., *et al* (2013): Diabetes mellitus triggers oxidative stress in the liver of alloxan-treated rats: a mechanism for diabetic chronic liver disease. Acta Cir Bras. 2013; 28(7): 502–508,

41. Alnahdi, H.S. (2018): The Possible Ameliorative Mechanisms of Curcumin and/or Coenzyme Q10 Against Hyperthyroidism Induced Liver Damage in Rats. Entomology and Applied Science Letters, 5(1), 7-16.

42. Mousa, H. S., Aal, S. M. A. and Abbas, N. A. (2018): Umbilical cord blood-mesenchymal stem cells and carvedilol reduce doxorubicin-induced cardiotoxicity: Possible role of insulin-like growth factor-1. Biomedicine and Pharmacotherapy, 105, 1192-1204.

43. Jörns, A., Tiedge, M. and Lenzen, S. (2002): Thyroxine induces pancreatic beta-cell apoptosis in rats. Diabetologia, 45(6): 851-855.

44. 44. Tögel, F., Weiss, K., Yang, Y., Hu, Z., Zhang, P. and Westenfelder, C. (2007): Vasculotropic, paracrine actions of infused mesenchymal stem cells are important to the recovery from acute kidney injury in Am J Physiol Renal Physiol., 292(5):1626- 1635.

45. Milanesi, A., Lee, J.W., Li, Z., Sacco, S., Villani, V., Cervantes, V., Perin, L. and Yu, J.S. (2012): Beta-Cell regeneration mediated by human bone marrow mesenchymal stem cells in PLoS ONE 7(8): e42177.

46. Fiorina, P., Jurewicz, M., Augello, A., Vergani, A., Dada, S., La Rosa, S., Selig, M., Godwin, J., Law, K., Placidi, C., Smith, R. N., Capella, C., Rodig, S., Adra, C. N., Atkinson, M., Sayegh, M. H. and Abdi, R. (2009): Immunomodulatory function of bone marrow-derived mesenchymal stem cells in experimental autoimmune type 1 diabetes in Journal of Immunology, 183(2): 993- 1004.

47. Bhansali, S., Kumar, V., Saikia, U., Medhi, B., Jha, V., Bhansali, A. and Dutta, P. (2015): Effect of mesenchymal stem cells transplantation on glycaemic profile and their localization in streptozotocin induced diabetic Wistar rats in Indian J Med Res 142: 63 -71.

48. Pagliuca, F. W., Millman, J. R., Gürtler, M., Segel, M., Van Dervort, A., Ryu, J. H., ... and Melton, D. A. (2014): Generation of functional human pancreatic β cells in *vitro*. Cell, 159(2), 428-439.

49. Zanini, C., Bruno, S., Mandili, G., Baci, D., Cerutti, F., Cenacchi, G., ... and Forni, M. (2011): Differentiation of mesenchymal stem cells derived from pancreatic islets and bone marrow into islet-like cell phenotype. PloS one, 6(12), e28175.

الملخص العربى

الدور العالجي للخاليا الجذعية في إصابة البنكرياس المستحث بفرط نشاط الغدة الدرقية لدى الجرذان البيضاء

كريمه فوزي عبد الفضيل، أسامه ياسين ابراهيم، مريم أحمد علي عبد المقصود، زينب منصور العزوني

قسم الهستولوجيا وبيولوجيا الخلية -كلية الطب البشرى- جامعة الزقازيق

المقدمة: يؤثر فرط نشاط الغدة الدرقية الغير منضبط سلبًا على جودة حياة المريض الجسديه.
الهدف من البحث: تقييم آلثار الضارة لفرط نشاط الغدة الدرقية على بنية البنكرياس لإناث البالغة من الجرذان البيضاء والدور العالجي للخاليا الجذعية الوسيطة لدم الحبل السري كإستراتيجية جديدة.
المواد وطرق البحث: تم تصنيف ٤٠ أنثى عذراء بالغة من الجرذان البيضاء إلى مجموعتين. الضابطة والمعالجة. تم تقسيم المجموعة المعالجة إلى مجموعتين فرعيتين ؛ فرط نشاط الغدة الدرقية ، وفرط نشاط الغدة الدرقية + الخاليا الجذعية. تم إجراء التحليل المصلي لتقييم وظائف الغدة الدرقية والبنكرياس والاجهاد التأكسدي وتحليل بيروكسيد الدهون. تمت معالجة عينات البنكرياس للفحص المجهري الضوئي. تم إجراء الفحص الكيميائي المناعي لبروتين الأنسولين و caspase-٣ و PCNA و CD١٠٥.
النتائج: أدى فرط نشاط الغدة الدرقية إلى تغيرات نسيجية وكيميائية حيوية في أنسجة البنكرياس. ظهرت أسيني مع السيتوبالزم المفرغ والنواة الداكنة. كانت الخلايا االلتهابية موجودة في الحاجز الواسع ولوحظ أيًضا العديد من ألياف الكولاجين. انخفاض كبير في هرمون TSH ، زيادة في نسبة الجلوكوز في الدم والاميليز في الدم ، وانخفاض في مستويات الانسولين في الدم ، وانخفاض معنوي في نشاط إنزيمات SOD وزيادة معنوية في مستوى MDA في مجموعة فرط نشاط الغدة الدرقية مقارنة بمجموعات الضبط. قامت الخلايا الجذعية الوسيطة في دم الحبل السري للانسان بتعديل هذه التغييرات وكشفت عن بنية شبه طبيعية و تم تغيير العلامات المصلية والأكسدة بشكل ملحوظ.
الاستنتاج: فرط نشاط الغدة الدرقية أثر بشكل خطير على التركيب النسيجي للبنكرياس مع اضطراب الحق في العلامات البيوكيميائية. كانت الخلايا الجذعية الوسيطة لدم الحبل السري البشري فعالة في تخفيف فرط نشاط الغدة الدرقية الناجم عن إصابة البنكرياس والتغيرات الكيميائية الحيوية في إناث الجرذان البيضاء البالغة.